Predicted Liquefaction in the Greater Oakland Area and Northern Santa Clara Valley During a Repeat of the 1868 Hayward Fault (M6.7-7.0) Earthquake

by
Thomas L. Holzer[1], Thomas E. Noce[2], and Michael J. Bennett[3]

ABSTRACT

Probabilities of surface manifestations of liquefaction due to a repeat of the 1868 (**M**6.7-7.0) earthquake on the southern segment of the Hayward Fault were calculated for two areas along the margin of San Francisco Bay, California: greater Oakland and the northern Santa Clara Valley. Liquefaction is predicted to be more common in the greater Oakland area than in the northern Santa Clara Valley owing to the presence of 57 km^2 of susceptible sandy artificial fill. Most of the fills were placed into San Francisco Bay during the first half of the 20th century to build military bases, port facilities, and shoreline communities like Alameda and Bay Farm Island. Probabilities of liquefaction in the area underlain by this sandy artificial fill range from 0.2 to ~0.5 for a **M**7.0 earthquake, and decrease to 0.1 to ~0.4 for a **M**6.7 earthquake. In the greater Oakland area, liquefaction probabilities generally are less than 0.05 for Holocene alluvial fan deposits, which underlie most of the remaining flat-lying urban area. In the northern Santa Clara Valley for a **M**7.0 earthquake on the Hayward Fault and an assumed water-table depth of 1.5 m (the historically shallowest water level), liquefaction probabilities range from 0.1 to 0.2 along Coyote and Guadalupe Creeks, but are less than 0.05 elsewhere. For a **M**6.7 earthquake, probabilities are greater than 0.1 along Coyote Creek but decrease along Guadalupe Creek to less than 0.1. Areas with high probabilities in the Santa Clara Valley are underlain by young Holocene levee deposits along major drainages where liquefaction and lateral spreading occurred during large earthquakes in 1868 and 1906.

INTRODUCTION

Liquefaction is commonly reported and frequently is a significant cause of damage during earthquakes in the San Francisco Bay Region. Liquefaction was reported during the 1868 Hayward Fault, 1906 San Francisco, and 1989 Loma Prieta earthquakes. While reports of ground failure during the 1868 earthquake are incomplete, photos and descriptions indicate some liquefaction occurred in San Francisco and in the south bay (Lawson, 1908). Its impact was modest presumably owing to the sparser settlement at the time. By contrast, liquefaction was extensive in areas of "made ground" in San Francisco in 1906, by which time extensive filling along the bay margin with loose sand had been done (Youd and Hoose, 1978). The associated ground deformation was responsible for the disruption of the water-supply system that ultimately enabled the damaging and costly conflagration in San Francisco to burn out of control for three days. In addition, extensive liquefaction was photographed and reported along the flood plain of Coyote Creek in the south bay. By the time of the 1989 earthquake, sandy artificial fills were also widespread along the shoreline in the east bay. These fills along with the older sandy fills in San Francisco exhibited extensive liquefaction (Holzer, 1998). No liquefaction was reported in the south bay.

This paper estimates probabilities of surface manifestations of liquefaction in the greater Oakland area and the northern part of the Santa Clara Valley (fig. 1) for a repeat of an earthquake like that on the Hayward Fault in 1868. The two study areas are located along the margin of San Francisco Bay, CA. The purpose of this paper is to assess the liquefaction hazard in these two areas when an earthquake like the 1868 event recurs. Its mean recurrence interval, based on a 12-earthquake chronology, is 161 yr (Lienkaemper and others, 2009). The methodology in this investigation is the same as that used by Holzer and others (2009) for liquefaction scenarios in the Santa Clara Valley. The methodology relies on complementary frequency distributions of the liquefaction potential index (LPI) to produce liquefaction probability curves that are a function of peak ground acceleration (PGA) and earthquake magnitude (**M**). PGA in this investigation was estimated with the new NGA ground-motion prediction equation of

[1] Thomas L. Holzer, U.S. Geological Survey, 345 Middlefield Road MS977, Menlo Park, California 94025, tholzer @usgs.gov
[2] Thomas E. Noce, tnoce@usgs.gov
[3] Michael J. Bennett, mjbennett@usgs.gov

Boore and Atkinson (2008). Based on PGA and **M**, the spatial pattern of liquefaction probabilities was then estimated with the liquefaction probability curves for the appropriate surficial geology. Computations were performed with ArcGIS® ModelBuilder.

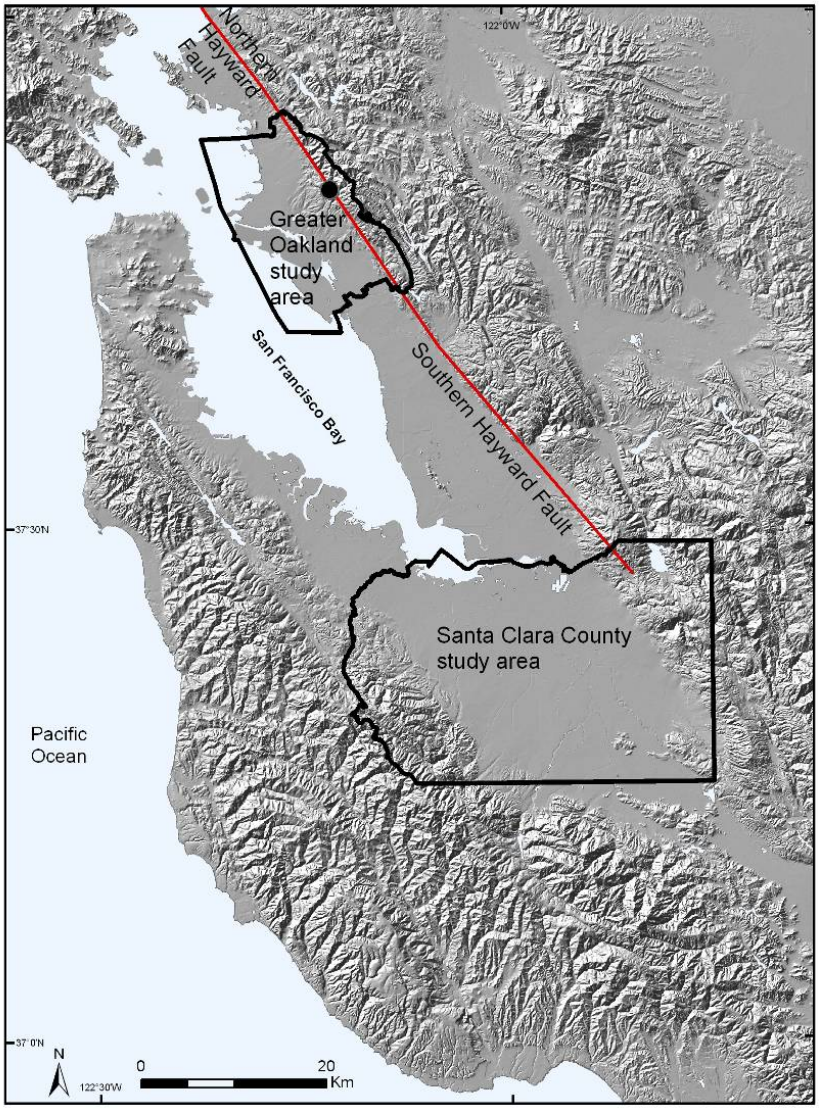

Figure 1. Locations of study areas and Hayward Fault in San Francisco Bay region, CA. Northern and southern segments of the fault are labeled (see black dot). Segment boundaries are from WGCEP (2003).

ENGINEERING GEOLOGY

Surficial Geology

In this investigation, we relied on surficial geologic mapping by Witter and others (2006) to delineate the regional distribution of geologic units. Their mapping was conducted at a 1:24,000 scale and offers a bay-area-wide consistent set of surficial geologic units. The stratigraphic relations of surficial geologic units and their liquefaction potential were assessed by extensive cone penetration test (CPT) soundings. CPT data are available at http://earthquake.usgs.gov/regional/nca/cpt/data/.

The Santa Clara Valley study area lies at the southern end of San Francisco Bay. It includes the communities of San Jose, Campbell, Cupertino, Los Altos, Los Gatos Milpitas, Mountain View, Palo Alto, Santa Clara, Saratoga, and Sunnyvale. The surficial geology of the study area is shown in figure 2. The valley is basically a trough that has been subsiding and filling with sediment during the Quaternary Period. Deposition of Quaternary alluvial fan and fluvial sediments has been influenced by both tectonic subsidence and climatic changes (Wentworth and Tinsley, 2005).

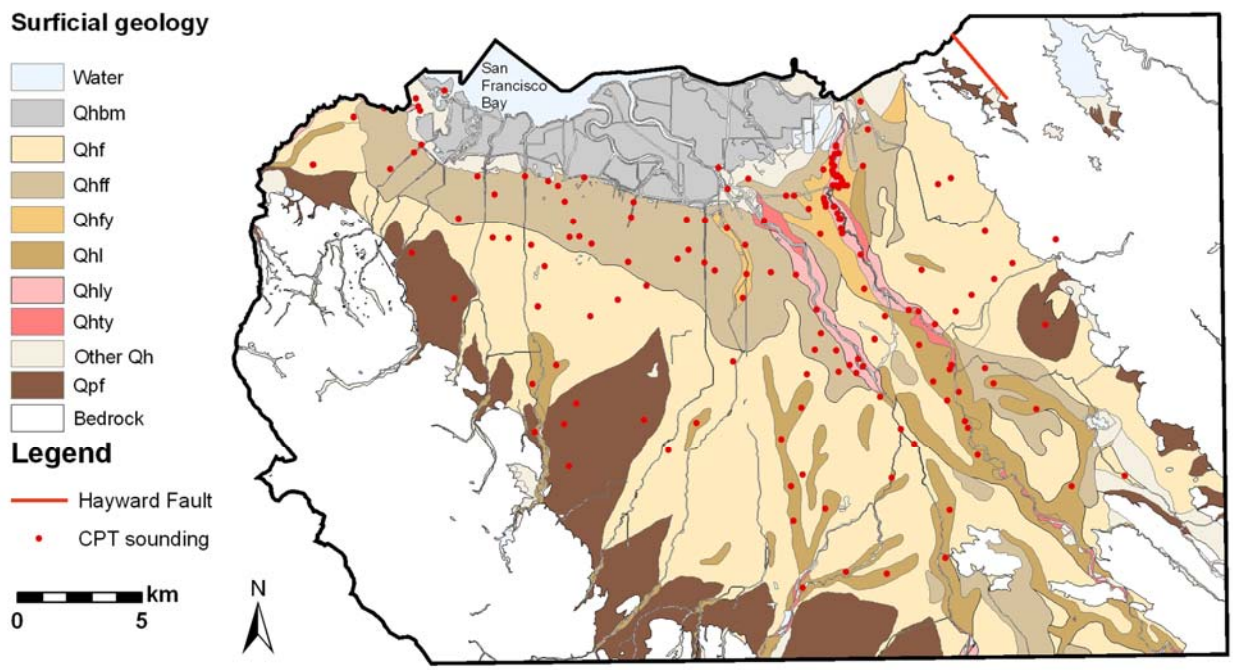

Figure 2. Surficial geology of northern Santa Clara Valley with CPT locations. Map unit designations beginning with "Qh" consist of Holocene alluvial fan and stream deposits and younger bay mud; Qhly denotes young Holocene levee deposits; and Qpf denotes Pleistocene alluvial fan deposits (Simplified from Witter and others, 2006). (Color figure available in CD/Web version.)

The surficial geology as mapped by Witter and others (2006) map indicates that the valley floor is blanketed by Holocene alluvial fan deposits (fig. 2). These deposits have an average thickness in the central part of the study area of approximately 9 m and a maximum thickness of 18 m (Holzer and others, 2009).

The surficial geology in figure 2 has been simplified from the mapping by Witter and others (2006) to emphasize the major units that were considered in the liquefaction hazard mapping. Their original surficial geologic map identified 18 Holocene map units, but it was not practical to explore all of the minor units because of site access limitations. To make the liquefaction hazard map, minor units were grouped with the major unit with which we anticipated they would have the greatest similarity based on their geologic descriptions. Witter and others (2006) identified three major Holocene fan units: Qhfy, a coarser grained facies around the margin of the valley associated with the heads of the alluvial fans; Qhff, a finer grained facies that is the distal end of the fans; and Qhly/Qhl, levee deposits along modern creeks. The areas mapped as young Holocene levee deposits also presumably include areas with buried Holocene channel and point bar deposits. In addition, Witter and others (2006) mapped a large area of younger bay mud, Qhbm, around the margin of San Francisco Bay. This area was not explored for hazard mapping purposes because it was mostly inaccessible. The simplified map in figure 2 also does not distinguish among Pleistocene alluvial fan deposits mapped by Witter and others (2006). These deposits are identified here simply as Qpf.

The greater Oakland study area lies along the coastal plain of eastern San Francisco Bay. In this investigation it includes the cities of Alameda, Berkeley, Emeryville, Oakland, and Piedmont. The surficial geology of the 140-km^2 study area is shown in figure 3. The area contains 5 major surficial geologic units in addition to

bedrock: artificial fill, younger San Francisco bay mud, Holocene alluvial fan deposits, Merritt Sand, and Pleistocene alluvial fan deposits.

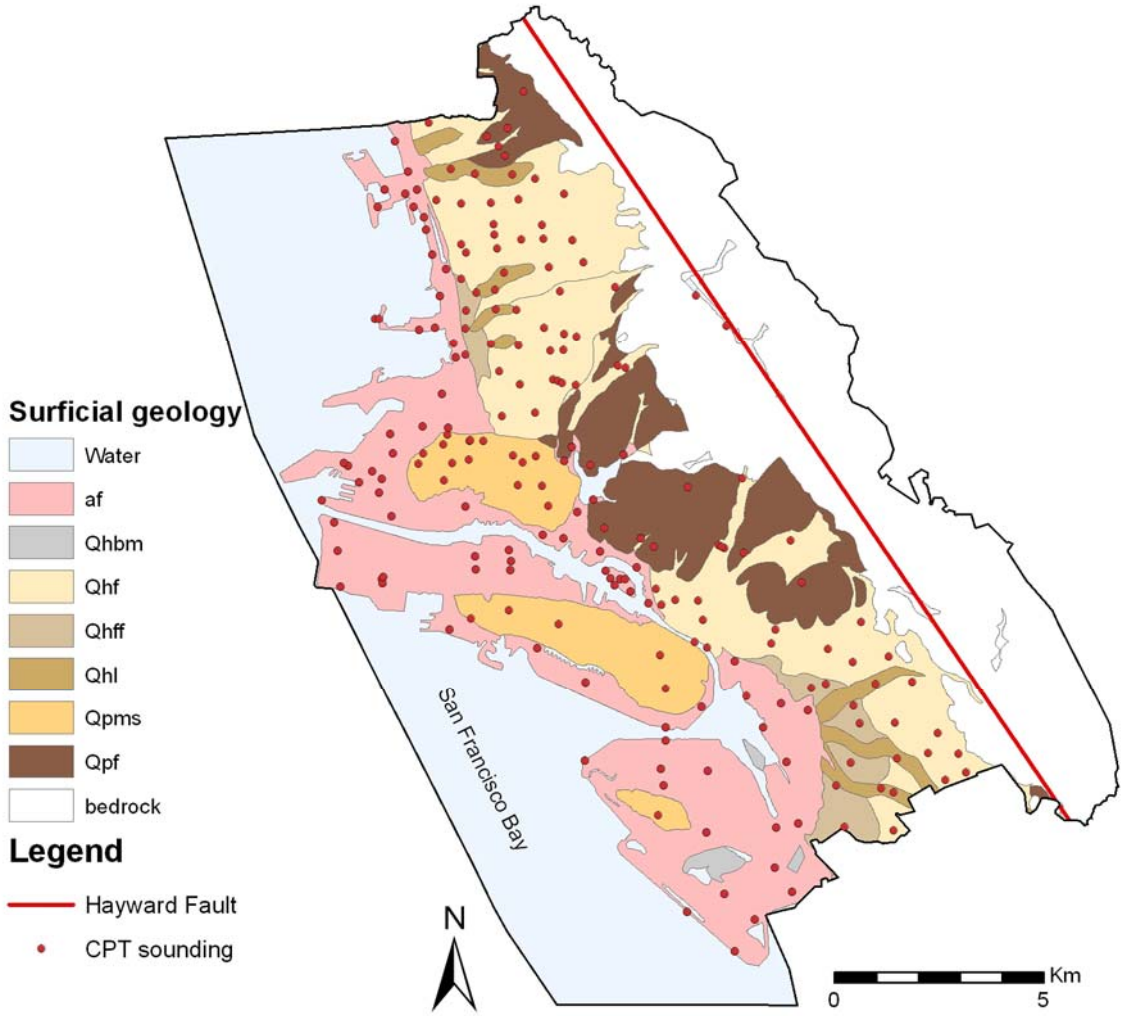

Figure 3. Surficial geology of greater Oakland area with CPT locations. Geologic units include: af, artificial fill; Qhbm, younger bay mud; Qhl, Qhf, and Qhff, Holocene alluvial fan deposits; Qpms, Merritt Sand; and Qpf, Pleistocene alluvial fan deposits (Simplified from Witter and others, 2006). (Color figure available in CD/Web version.)

The sandy artificial fills were emplaced before 1964 by either hydraulic dredging or dumping from land. Most of the fill was emplaced without consideration for its vulnerability to liquefaction, although soils have been improved at some sites. According to Holzer and others (2006a), fill thickness ranges from approximately 11 m to zero, where the fill pinches out along the original shoreline. Average thickness is approximately 3 m. The Holocene alluvial fan deposits generally consist of fine-grained deposits, although fluvial sands locally are present. Thickness of the fan deposits ranges from approximately 14.3 m to zero, where they overlap deposits of Pleistocene age. Average thickness is 4.4 m. These fan deposits rest on older Pleistocene alluvial fan deposits whose upper surface is heavily dissected as the result of tectonic uplift and stream incision. The Merritt Sand, which is predominantly a wind-blown deposit, locally overlies the Pleistocene alluvial fan deposits as well as older bay deposits. The Merritt Sand was chiefly deposited during and near the end of the Pleistocene Epoch when sea level was below its current level. Ground water is presently encountered at less than 3 m depth in much of the study area.

1868 Hayward Earthquake

The 1868 Hayward earthquake was used for the liquefaction scenarios described in this investigation. The earthquake predates instrumental recordings and its magnitude must be inferred from approximate rupture area, seismic intensity reports, and geodetic displacements. For the scenarios, we considered magnitudes ranging from **M**6.7 to **M**7.0. The lower magnitude is the consensus median estimate of the 2002 U.S. Geological Survey working group (WGCEP, 2003), and the higher magnitude is the estimate of Yu and Segall (1996), which was based on contemporaneous geodetic measurements. Historical descriptions (Lawson, 1908) of the surface rupture suggest that the 1868 earthquake occurred on the southern segment of the Hayward Fault (fig. 1).

METHODOLOGY

Liquefaction Prediction

In this investigation as in our earlier mapping efforts (Holzer and others, 2006a; Holzer and others, 2009), we used LPI as defined by Iwasaki and others (1978) to estimate the variability of liquefaction potential of surficial geologic units. As proposed by Iwasaki and others (1978), LPI weighs liquefaction factors of safety and thickness of potentially liquefiable layers for a sounding or boring according to depth. It assumes that the severity of liquefaction is proportional to:

1. cumulative thickness of the liquefied layers;
2. proximity of liquefied layers to the land surface; and
3. amount by which the liquefaction factor of safety (FS) is less than 1.0, where FS is the ratio of the soil capacity to resist liquefaction to seismic demand imposed by the earthquake.

Iwasaki and others (1978) defined LPI as:

$$LPI = \int_0^{20m} F\, w(z)\, dz \qquad (1)$$

where

$F = 1 - \mathrm{FS}$ for $\mathrm{FS} \leq 1$ (2a)

$F = 0$ for $\mathrm{FS} > 1$ (2b)

$w(z) = 10 - 0.5\, z$, where z is the depth in meters. (2c)

The weighting factor, $w(z)$, ranges from ten at the surface to zero at 20 m (Iwasaki and others, 1978). $F = 0$ above the water table. LPI values can theoretically range from 0 to 100. For a more extensive discussion of LPI and its application to liquefaction hazard mapping, the reader is referred to Holzer (2008). Figure 4 illustrates the application of equation 1 to a CPT sounding in the greater Oakland area. The dashed lines in figure 4 indicate the accumulation of LPI for 3 different PGA values caused by an **M**7.0 earthquake. LPI for the sounding increases from 0.2 to 13.5, respectively, as PGA increases from 0.1 to 0.5 g. The sandy artificial fill near the land surface and below the water table is the primary contributor to LPI.

FS was computed with the Seed-Idriss simplified procedure (Seed and others, 1985) as modified for the CPT by Robertson and Wride (1998). This is the procedure recommended by Youd and others (2001). This methodology is consistent with the calibration of LPI by Toprak and Holzer (2003), which relied on Robertson and Wride (1998) to compute FS. Toprak and Holzer (2003) evaluated the significance of LPI values by correlating LPI with surface manifestations of liquefaction. They observed that the median values of LPI were 5 and 12, respectively, in areas with sand boils and lateral spreads. Lower and upper quartiles were 3 and 10 for sand boils and 5 and 17 for lateral spreads.

In the mapping methodology developed by Holzer and others (2002), the probability of surface manifestations of liquefaction for each surficial geologic unit is derived from complementary cumulative frequency distributions of LPI. Distributions are computed for a specific earthquake magnitude and water table condition. By

computing distributions for different PGA values, probability as a function of PGA can be estimated for each unit based on the frequency at LPI ≥ 5. The procedure is illustrated in figure 5. Figure 5a shows LPI distributions of young Holocene levee deposits (Qhly) in the Santa Clara Valley assuming a 5-m-deep water table and a **M**7.0 earthquake. Each distribution is based on a specific PGA and the same 25 CPT soundings conducted in Qhly. The probability of liquefaction at each PGA is the frequency value at LPI≥ 5 for each distribution. Figure 5b shows the liquefaction probability as a function of PGA for an **M**7.0 earthquake. The probabilities were inferred from the frequency at LPI≥ 5 shown in figure 5a. This methodology is the same as that used to map liquefaction hazard in the greater Oakland area and Santa Clara Valley (Holzer and others, 2002; Holzer and others, 2006a; Holzer and others, 2006b; Holzer and others, 2009). Although the complementary cumulative frequency at LPI≥ 5 is interpreted here as the conditional probability of liquefaction at a randomly selected location within the area underlain by the geologic unit given an earthquake magnitude and PGA, it also can be interpreted as the percent area with surface manifestations of liquefaction (Holzer and others, 2006a).

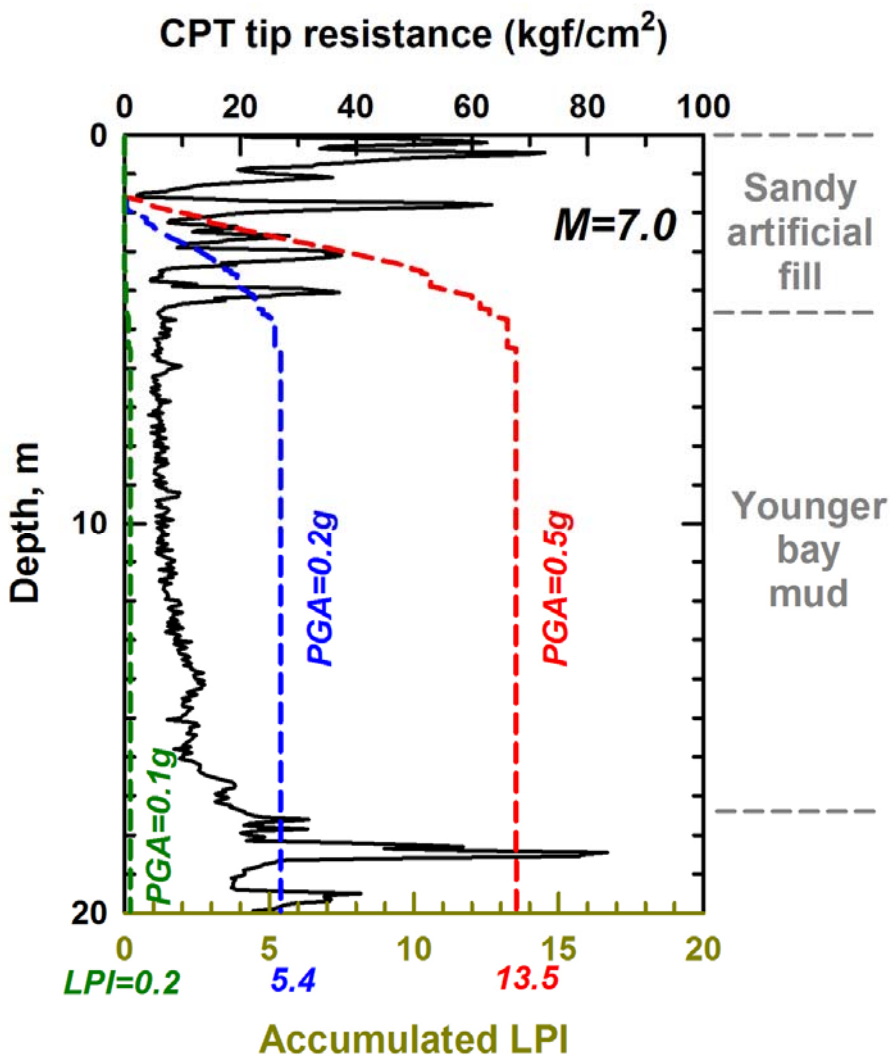

Figure 4. Example of LPI computations for CPT sounding ALC005 in sandy artificial fill in the greater Oakland area for an **M**7.0 earthquake and three levels of ground motion. (Color figure available in CD/Web version.)

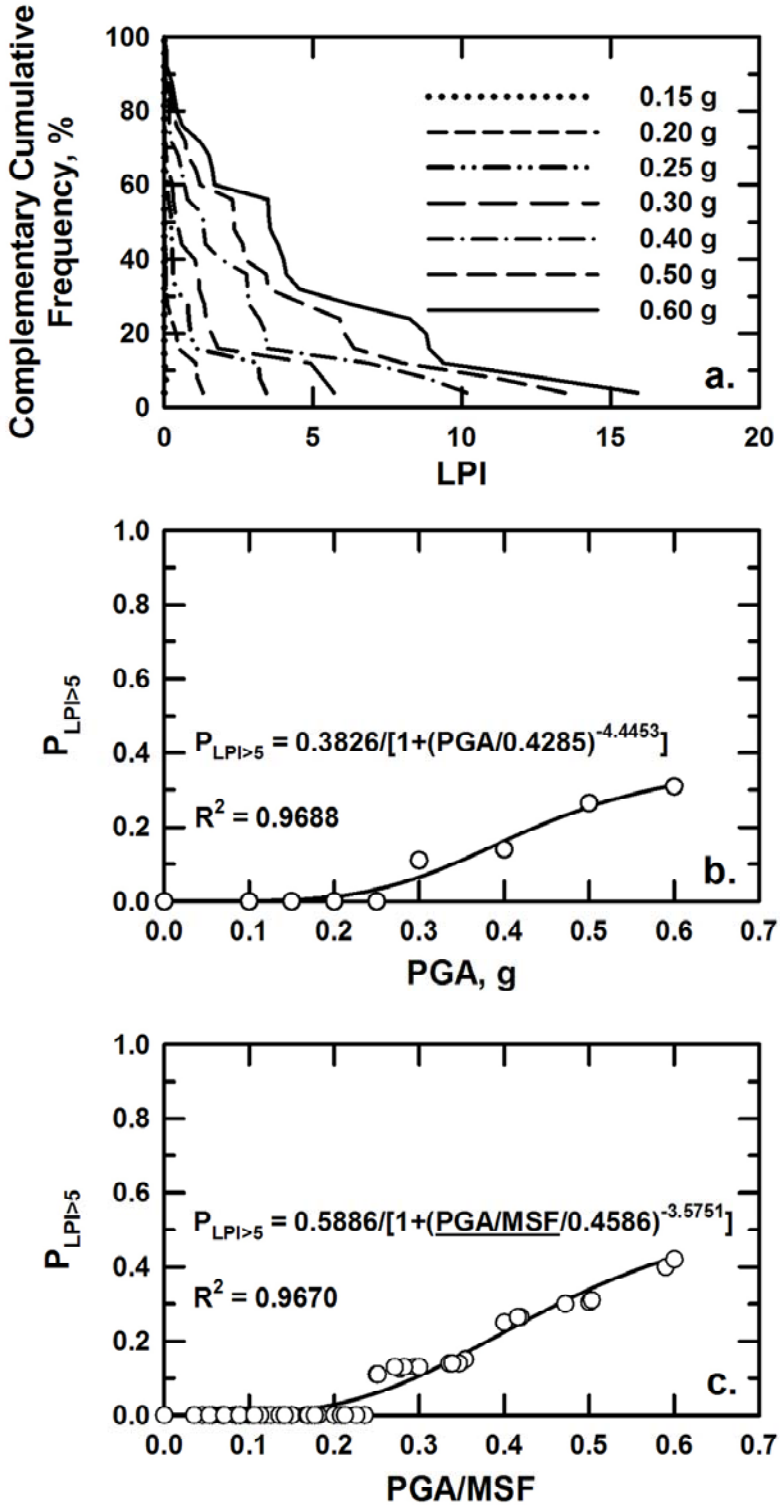

Figure 5. Liquefaction characteristics of young Holocene levee deposits (Qhly) in the Santa Clara Valley: (a) Complementary cumulative frequency distributions of LPI as a function of PGA for an **M**7.0 earthquake and a water table depth of 5 m; (b) Probability of surface manifestations of liquefaction for an **M**7.0 earthquake; and (c) Liquefaction probability curve. (Holzer and others, 2009, fig. 4)

Predicting the probability of liquefaction with spatially variable ground motions is computationally simplified by curve fitting the relation between probability and PGA. Holzer and others (2006b) recommended a 3-parameter logistic equation of the form shown in figure 5b. Rix and Romero-Hudock (2007) generalized the probability relation to other earthquake magnitudes by scaling the seismic demand (PGA) by the magnitude scaling factor (MSF) from the simplified procedure (fig. 5c). Data points in figure 5c are probabilities from complementary cumulative frequency distributions computed for $5.5 \leq \mathbf{M} \leq 8.0$ in 0.5 magnitude increments and $0 \leq$ PGA ≤ 0.6 g in 0.1 g increments. In the simplified procedure as described in Youd and others (2001), MSF = $10^{2.24}/\mathbf{M}^{2.56}$. Holzer (2008) recommended that the relation between liquefaction probability and magnitude-scaled PGA for a surficial geologic unit be referred to as the "liquefaction probability curve" (*e.g.*, fig. 5c).

The Robertson and Wride (1998) simplified procedure does not require soil samples for liquefaction evaluation. This is a convenient advantage when dealing with large numbers of CPT soundings as was the situation in this investigation. The procedure uses the soil behavior index, I_C, to predict soil behavior. I_C values are determined with the normalized and dimensionless cone tip resistance and friction ratio. For details of the normalization and nondimensionalization and the computation of I_C, the reader is referred to Robertson and Wride (1998). Values of I_C range from 1.64 or less for clean sands to values greater than 2.6 for silt mixtures and finer grained soils. Soils with $I_C > 2.6$ are not considered to be susceptible to liquefaction. In the procedure as implemented by Robertson and Wride (1998), an apparent fines correction based on I_C value is applied for soils with $1.64 < I_C < 2.6$.

As was extensively discussed by Holzer and others (2009), the implementation by Robertson and Wride (1998) of I_C can cause nonliquefiable soil to be misclassified as liquefiable, particularly for soils with $2.6 > I_C > 2.4$. Such misclassification appears to occur with Holocene alluvial fan deposits in both the greater Oakland area and northern Santa Clara Valley. To avoid (or at least decrease the incidence of) misclassifying nonsusceptible soils as susceptible in soundings without samples, Holzer and others (2009) modified the Robertson and Wride procedure to classify soils with $I_C > 2.4$ as nonsusceptible. This modification was adopted here for both the greater Oakland area as well as the northern Santa Clara Valley. For further discussion, the reader is referred to Holzer and others (2009). It is appropriate to note that this modification is consistent with the analysis by Suzuki and others (2003) of CPT data at 78 sites in Japan where liquefaction is known either to have or not to have occurred during earthquakes. Liquefaction was not observed at sites where $I_C > 2.4$.

Ground-motion Prediction

PGA was estimated with the new NGA ground-motion prediction equation by Boore and Atkinson (2008). Their empirical relation predicts PGA as a function of earthquake magnitude and mechanism, fault type, closest distance to the surface projection of the fault plane (R_{JB}), and local site amplification. For this investigation, both a strike-slip earthquake mechanism and vertical fault type were assumed. Thus, only differences in distance from the fault and local site conditions cause the spatial variations of PGA in the ground-motion estimates. Boore and Atkinson (2008) rely on the time-averaged shear-wave velocity to 30 m (V_{S30}) to predict site amplification.

Examples of ground-motion prediction curves for **M**6.7 and **M**7.0 earthquakes, the scenarios that were used in this investigation, are compared in figure 6a. The comparison is for a V_{S30} = 235 m/s site condition. The equations predict that the decrease of PGA with distance in the near field is very small. In addition, differences of PGA for **M**6.7 and **M**7.0 earthquakes in the near field are relatively small, ~3 %. Soil nonlinearity that Boore and Atkinson (2008) incorporated into their equation explains this small difference. The impact of nonlinearity on strong ground motion estimates is illustrated in figure 6b, which plots PGA at R_{JB} = 5 km for different values of V_{S30}. PGA values decrease significantly because of nonlinearity as V_{S30} decreases below 300 m/s.

The spatial variation of V_{S30} in the Santa Clara Valley was approximated by subdividing the area underlain by Holocene alluvial fan deposits into two subareas based on the historically shallowest ground water table (Holzer and others, 2009). Average values of V_{S30} were then computed for each subarea based on seismic CPT soundings. In the central subarea, the historically shallow water table was within 3 m of the land surface. In the surrounding subarea, the historically shallow water table was deeper than 3 m. Because most soundings were shallower than 30 m (average depth= 17.6 m), V_{S30} was estimated for each sounding by projecting the velocity measured at the bottom

of the sounding to 30 m. In the central subarea, only soundings with a depth that exceeded 15 m were used. In the surrounding subarea, only soundings that exceeded 10 m were used.

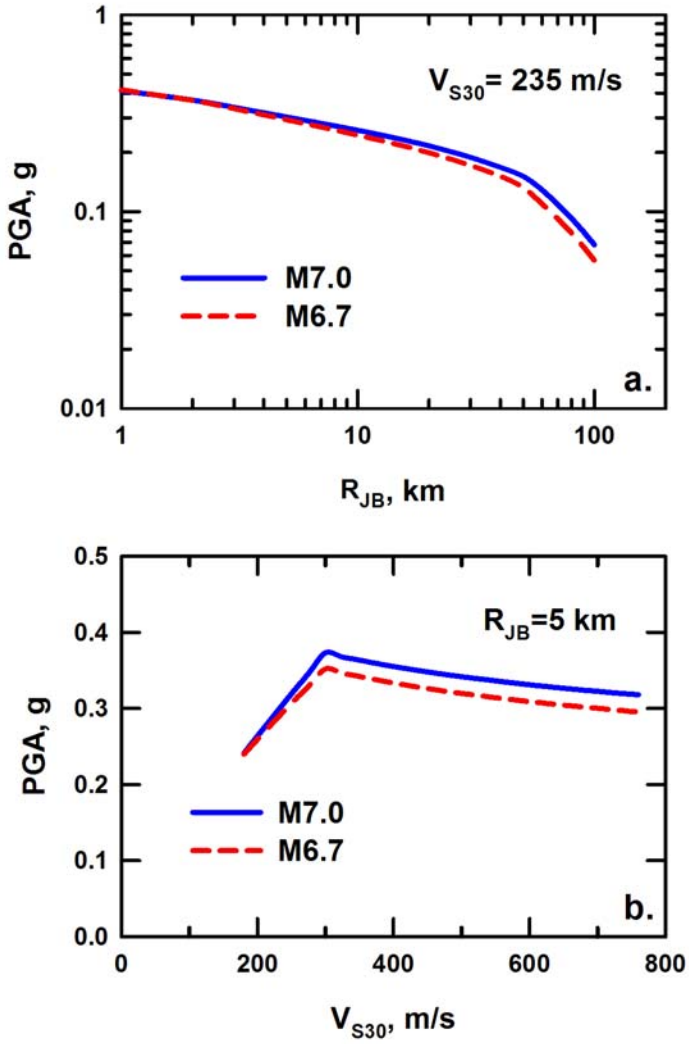

Figure 6. Median ground motion predicted by Boore and Atkinson (2008): (a) PGA as a function of distance from fault (R_{JB}) for sites with V_{S30} = 235 m/s, and (b) PGA at 5 km as a function of V_{S30}. (Holzer and others, 2009, fig. 8)

The map of V_{S30} in the greater Oakland area was based on the shallow velocity model described by Holzer and others (2005b). The map of V_{S30} was created by mapping the spatial variation of the thickness of Holocene sediment and artificial fill and then using average velocities of these units and underlying Pleistocene sediment to estimate the spatial variation of V_{S30}. The reason for this approach was that land surface at the end of the Pleistocene Epoch in the greater Oakland area was deeply incised by streams that had adjusted to the low stands of Pleistocene sea levels. Hand contouring of this old land surface produced a more geologically reasonable three-dimensional boundary between Holocene and Pleistocene sediments than did the surface implied by automated contouring of V_{S30} values.

Scenario Map Preparation

The liquefaction scenario maps were created with ArcGIS® ModelBuilder. Liquefaction probabilities and resulting maps were produced based on 4 input parameters: a shapefile of the surficial geology that was attributed with the liquefaction probability curve constants for each surficial geologic unit; a fault shapefile; a V_{S30} grid compiled from the seismic CPT soundings; and earthquake magnitude.

To compute a liquefaction scenario, ModelBuilder first created a grid of the study area with nodes at a 50-m spacing. Then ModelBuilder converted the grid into a point file, and built a table associated with the points. For each point, the table was populated with: (1) liquefaction probability curve constants appropriate to the surficial geology; (2) V_{S30} values; and (3) nearest distance to the surface projection of the Hayward Fault. The Boore and Atkinson (2008) ground motion prediction equation was used to compute PGA at each point based on the associated V_{S30} and fault distance. Once the table was populated with these PGA values, liquefaction probability was computed at each point based on earthquake magnitude and the liquefaction probability curve constants. Finally, an inverse distance weighted technique was used to turn the point file into a new 50-m grid with liquefaction probabilities within the study area.

LIQUEFACTION PROBABILITY CURVES

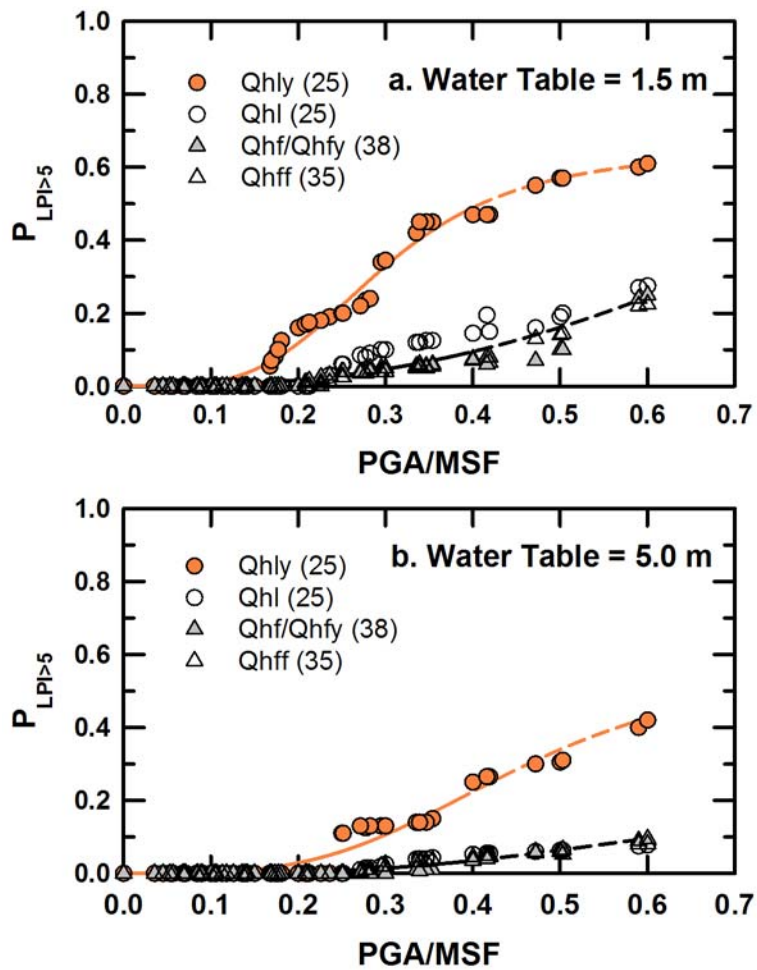

Figure 7. Liquefaction probability curves for alluvial fan deposits in the Santa Clara Valley: (a) Water table depth at 1.5 m; and (b) Water table depth at 5 m. Number of CPT soundings in each surficial geologic unit is shown in parentheses in the legends. See Table 1 for logistic regression equations.

Estimated probabilities of surface manifestations of liquefaction ($P_{LPI>5}$) of the major surficial geologic units in the Santa Clara Valley are shown in the upper and lower panels, respectively, of figure 7 for two water table depths, 1.5 and 5 m. Probabilities are based on the frequencies at LPI> 5 of the complementary cumulative frequency distributions for each surficial unit, using an $I_C \geq 2.4$ criterion to identify nonsusceptible soil.

Liquefaction probability curves for the major Holocene alluvial fan units in general are similar except for Qhly, the young Holocene levee deposits. The liquefaction probabilities of Qhly are significantly higher than the other Holocene alluvial fan units (fig. 7). Probabilities of surface manifestations of liquefaction of the other units in

general are modest except for the 1.5-m-deep water table and at high levels of ground motion (PGA > 0.4 g) (fig. 7a). The contrast in liquefaction probabilities between Qhly and the other units is even greater for the 5-m-deep water table (fig. 7b). Because liquefaction probability curves for all of the Holocene fan units except for Qhly are similar, curves for the non-Qhly units were combined to create a single curve. In addition to the obvious simplification for the map making process, there is a statistical argument to combine the units. When the LPI-based liquefaction probability of a geologic unit is small, the number of CPT soundings in the unit becomes an issue. For example, liquefaction probabilities of less than 0.05 in units with only 20 soundings are not statistically robust. By combining the units, Qhl, Qhf/Qhfy, and Qhff, into a single curve, the 98 soundings provide a more robust estimate of the liquefaction probability. The regression equations obtained by fitting a three-parameter logistic curve to these data are given in Table 1.

Table 1. Logistic regression equations for liquefaction probability curves, Santa Clara Valley

Water table depth, m	Qhly	Qhf, Qhff, and Qhl
1.5	$\dfrac{0.6503}{1+\left[\dfrac{PGA/MSF}{0.2981}\right]^{-3.7789}}$	$\dfrac{1.8336}{1+\left[\dfrac{PGA/MSF}{1.2479}\right]^{-2.5577}}$
5.0	$\dfrac{0.5886}{1+\left[\dfrac{PGA/MSF}{0.4586}\right]^{-3.5751}}$	$\dfrac{0.2268}{1+\left[\dfrac{PGA/MSF}{0.6571}\right]^{-3.4305}}$

Estimated probabilities of surface manifestations of liquefaction of the major surficial geologic units in the greater Oakland area are shown in figure 8 for a water table depth of only 1.5 m. A curve for only one water table depth was needed for mapping as is described in the following section. Not unexpectedly the sandy artificial fills (af) are substantially more liquefiable than the Holocene alluvial fan deposits in the greater Oakland area. The liquefaction probabilities for the Holocene alluvial fan units–Qhf, Qhff, and Qhl–were similar so these units were lumped together as a single unit for the purpose of computing the liquefaction probability curve. The regression equations for the liquefaction probability curves are given in Table 2.

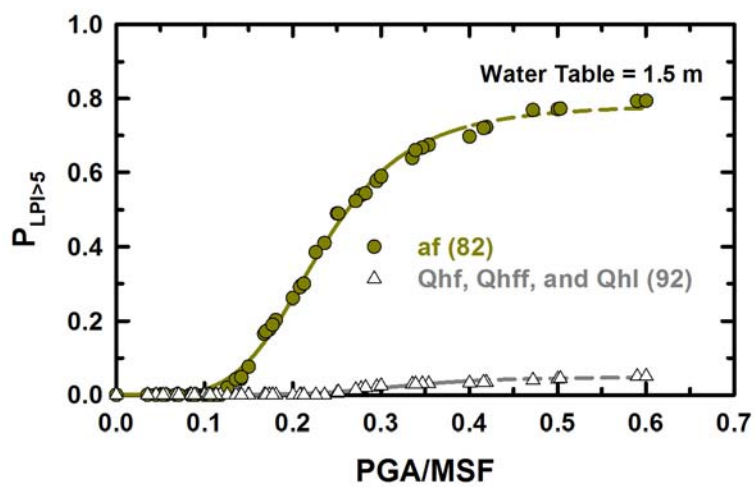

Figure 8. Liquefaction probability curves for sandy artifical fill (af) and alluvial fan deposits (Qhf, Qhff, and Qhl) in the greater Oakland area for a water table depth of 1.5 m. Number of CPT soundings in each surficial geologic unit is shown in parentheses in the legend. See Table 2 for logistic regression equations.

Table 2. Logistic regression equations for liquefaction probability curves, greater Oakland area

Water table depth, m	af	Qhf, Qhff, and Qhl
1.5	$\dfrac{0.7835}{1+\left[\dfrac{PGA/MSF}{0.2319}\right]^{-4.6302}}$	$\dfrac{0.0479}{1+\left[\dfrac{PGA/MSF}{0.3233}\right]^{-6.0539}}$

The reliability of predicted probabilities for the Pleistocene alluvial fan deposits is questionable as will be discussed, and we did not attempt to assess the hazard posed by these deposits in either the Santa Clara Valley or greater Oakland areas. Some investigators have questioned the direct application of the field-based simplified procedure to pre-Holocene deposits because it may be overly conservative when applied to older deposits. The simplified procedure is based on case histories that include only Holocene deposits. These investigators (*e.g.*, Leon and others, 2006) have proposed using age corrections when applying the simplified procedure to older deposits. In addition to these methodological concerns, liquefaction of Pleistocene deposits in California has not been reported in historical earthquakes. Although liquefaction of these deposits cannot be precluded because liquefaction of deposits of Pleistocene age has been reported in earthquakes in the central and eastern United States (Obermeier and others, 1990), probabilities were not assigned to areas underlain by these deposits.

SCENARIO MAPS

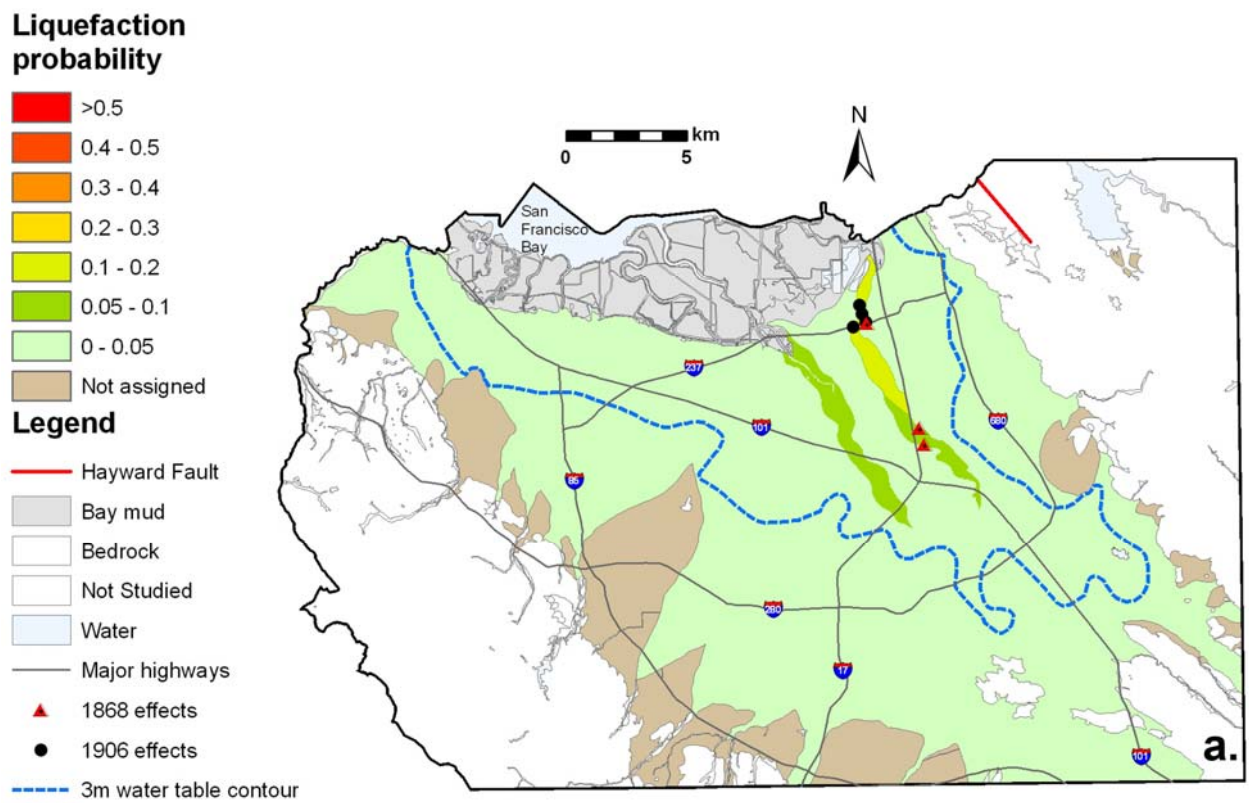

Figure 9a. Map of liquefaction probabilities for the northern Santa Clara Valley for **M**6.7 earthquake. Geographic Information System (GIS) files for this map are published (Holzer and others, 2008). (Color figure available in CD/Web version.)

Maps of liquefaction probability are shown in figures 9 and 10, respectively, for the Santa Clara Valley and the greater Oakland area. Because of the uncertainty of the earthquake magnitude, maps were produced for both **M**6.7 and **M**7.0.

The selection of a water-table depth with which to compute the liquefaction hazard for the Santa Clara Valley is an important issue. Both ground water and surface water in the Santa Clara Valley are managed by the Santa Clara Valley Water District. Thus, the water table is subject to anthropogenic influence. This and annual rainfall variations cause the water table to fluctuate significantly from periods of extended drought compared to periods of high rainfall. Accordingly, liquefaction hazard varies as the water table fluctuates with the hazard being lower during droughts than wet years. Defining the liquefaction hazard in the Santa Clara Valley is further challenged by the absence of detailed and contemporaneous regional data showing depth to the water table.

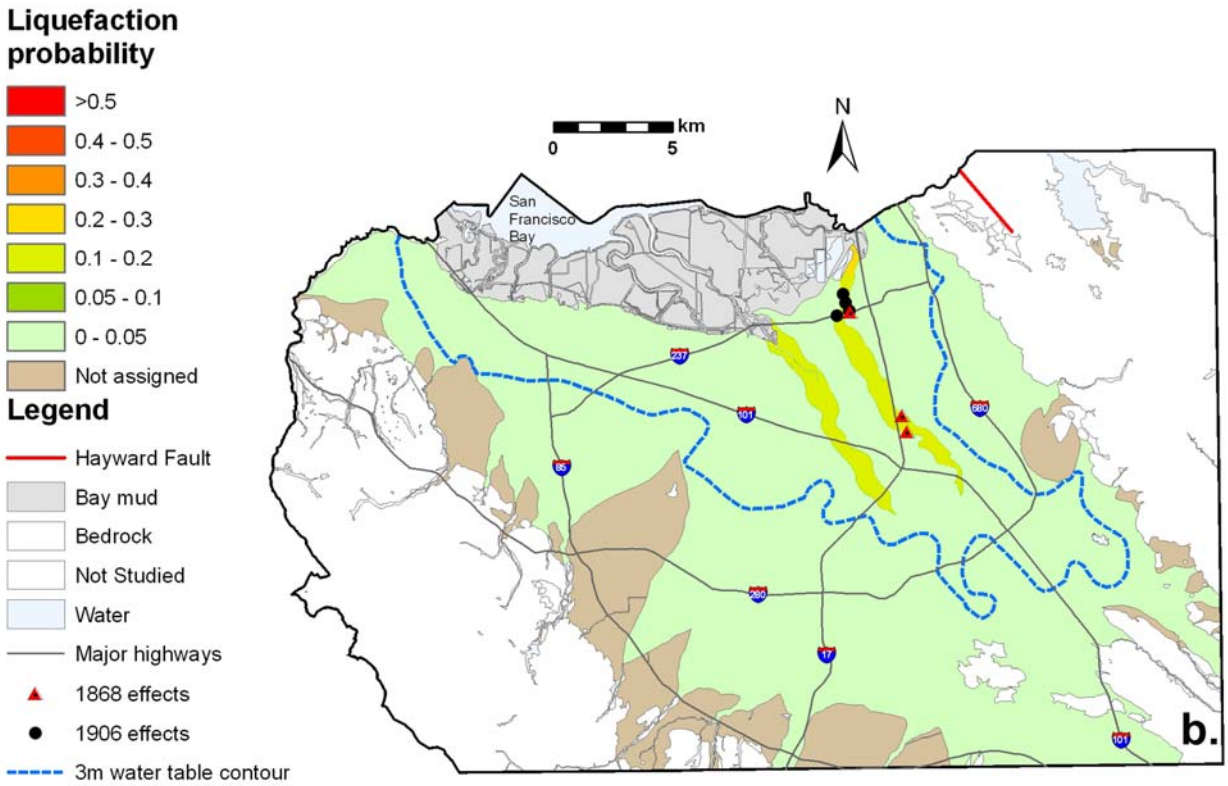

Figure 9b. Map of liquefaction probabilities for the northern Santa Clara Valley for **M**7.0 earthquake. (Color figure available in CD/Web version.)

To incorporate the effect of water-table depth on the hazard in the Santa Clara Valley, we relied on a map of the historically shallowest water table that was prepared by the California Geological Survey (CGS) as part of its regulatory seismic hazard mapping of the valley (http://gmw.consrv.ca.gov/shmp/html/pdf_maps_no.html). They produced the map of the water table by using the shallowest water table observed in borings drilled over many decades. Although not a hydrologic snapshot of the water table, the map at least approximately portrays the shallowest water table condition that is likely to be encountered over time within the study area. It therefore yields a conservative (*i.e.*, highest liquefaction probability) hazard map. To computationally simplify the prediction of liquefaction probability in this investigation, the map of the historically shallowest water table was divided into two subareas separated by the 3-m (10-ft) contour of depth to the water table. This contour is shown in figure 9 as a dashed blue line. Within and outside this contour, respectively, the liquefaction probability curves for water-table depths of 1.5 and 5 m were applied.

Consultant reports with irregular monitoring observations at leaking underground storage tanks in the study area, which are compiled at the Santa Clara Valley Local Oversight Program Public Record Document Search web site (http://lustop.sccgov.org), permit comparison of current and historically shallowest water-table conditions. A selective review of these reports suggests that the current water table is near its historically shallow position at least in the central subarea. In addition, the reports suggest that the water table seasonally fluctuates only approximately 0.5 m in this area. Thus, even though generally conservative, the hazard maps of the central subarea approximate the current level of liquefaction hazard. Because the historically shallow water tables are substantially deeper than 5 m in most of the subarea outside of the 3-m contour, the hazard maps in this subarea presumably are very conservative.

In the northern Santa Clara Valley, for a **M**7.0 earthquake and the assumed water-table depth of 1.5 m–the historically shallowest water level–in the central part of the valley, liquefaction probabilities range from 0.1 to 0.2 along Coyote and Guadalupe Creeks, but are less than 0.05 elsewhere. For a **M**6.7 earthquake, probabilities remain greater than 0.1 along Coyote Creek but decrease along Guadalupe Creek to less than 0.1. The higher probabilities are in areas underlain by young Holocene levee deposits (Qhly) where liquefaction and lateral spreading were reported following both the 1868 Hayward and 1906 San Francisco **M**7.8 earthquakes.

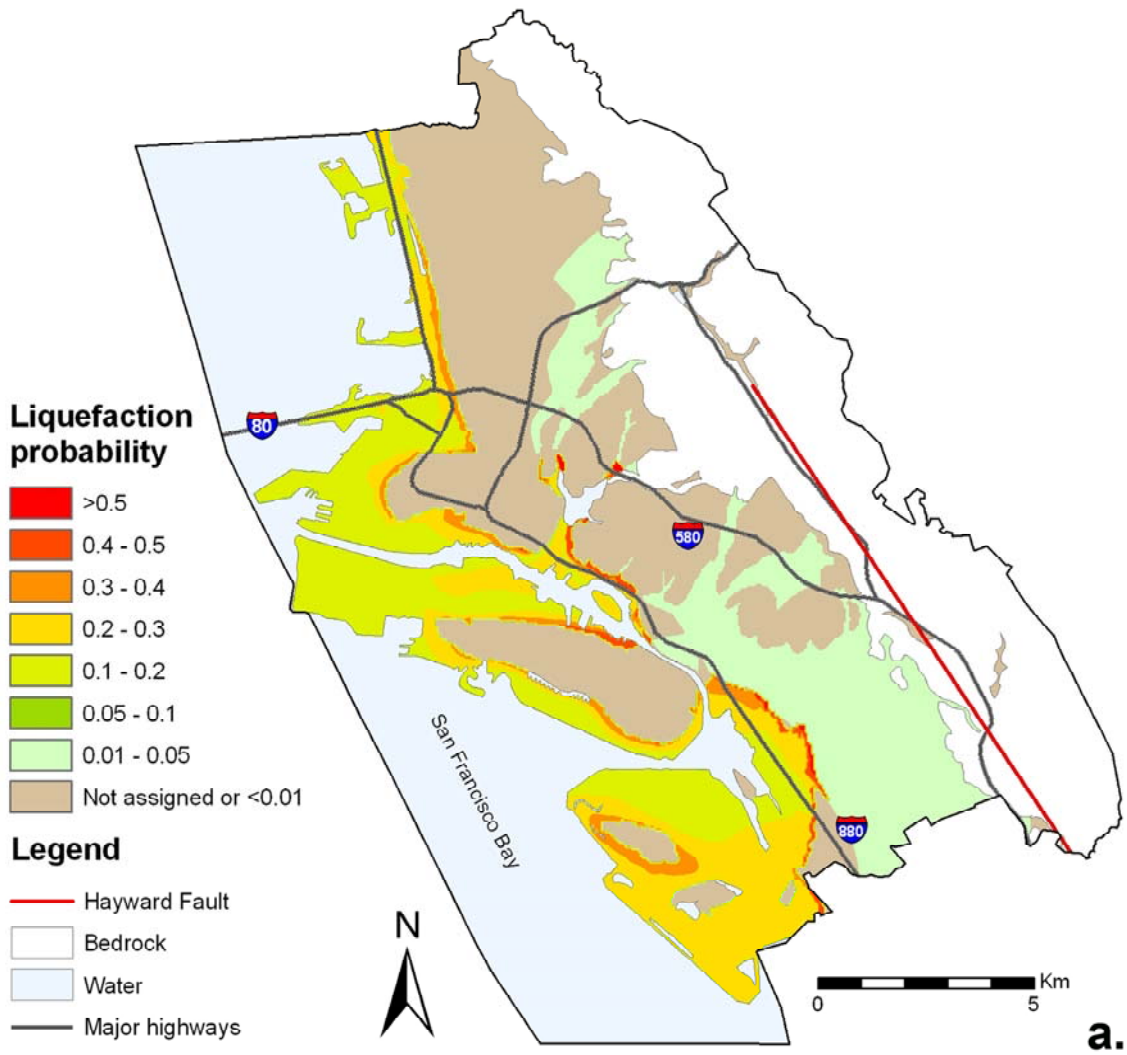

Figure 10a. Map of liquefaction probabilities for the greater Oakland area for **M**6.7 earthquake. (Color figure available in CD/Web version.)

The water table in the greater Oakland area unlike the Santa Clara Valley is essentially unaffected by pumping. In addition, because CPT sounding holes were not grouted, we were able to measure depth to the water table upon completion of most soundings. Water levels in the flat lying area of sandy artificial fill are fairly shallow and stable because of its uniform elevation and proximity to San Francisco Bay. Depth to the water table averaged 1.59 (±0.64) m in this area. In the area underlain by the Holocene alluvial fan deposits, depth to the water table averaged 3.10 (±1.21) m; measured values ranged from 1.10 m at lower elevations to 6.10 m at higher elevations. To produce a conservative hazard map for the greater Oakland hazard area, we assumed a constant water-table depth of 1.5 m.

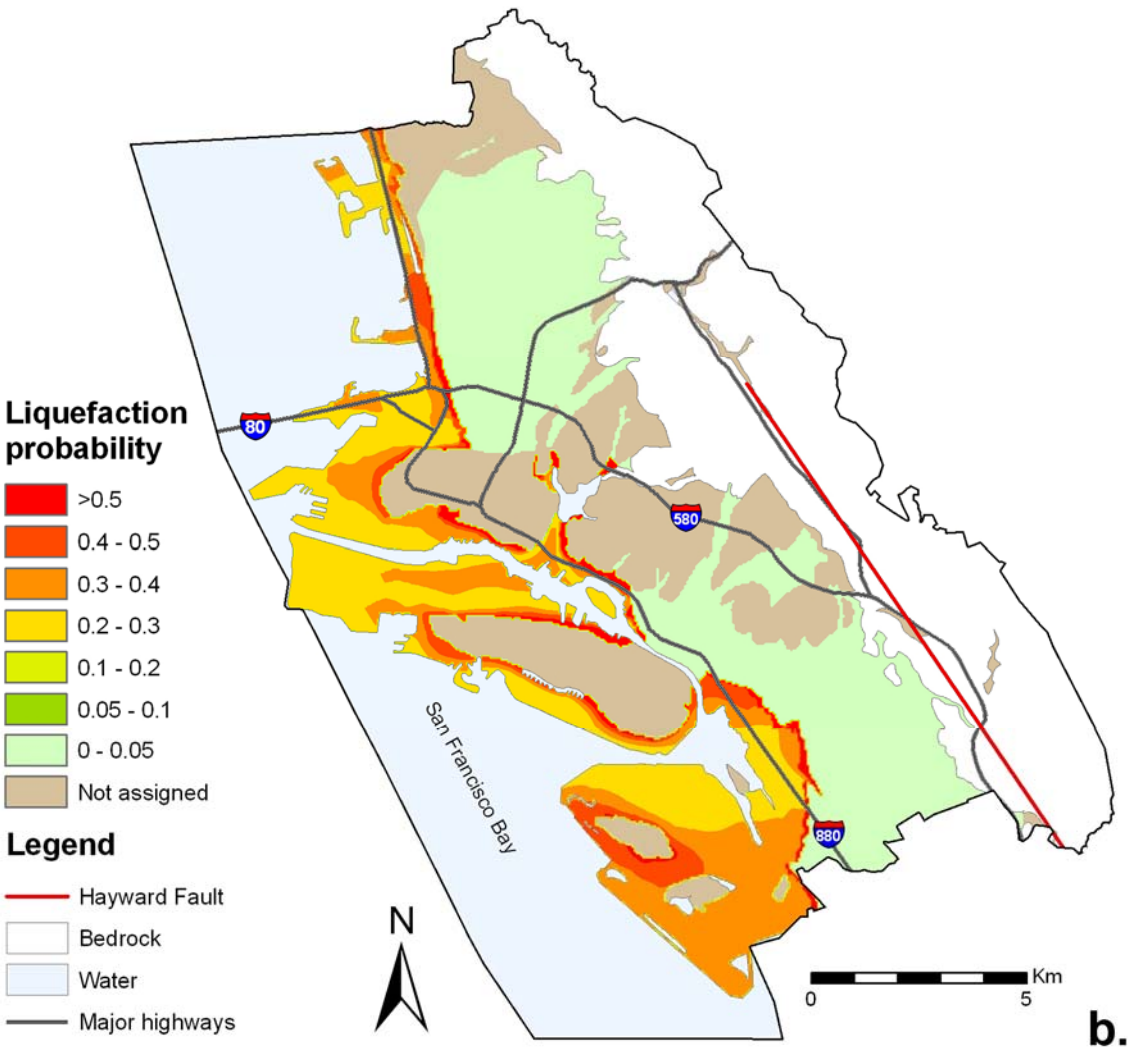

Figure 10b. Map of liquefaction probabilities for the greater Oakland area for **M**7.0 earthquake. (Color figure available in CD/Web version.)

The resulting maps of liquefaction probability indicate that the liquefaction hazard in Oakland is greatest in the 57 km^2 area of sandy artificial fill (figs. 3 and 10). Most of the fills were placed in San Francisco Bay during the first half of the 20th century before liquefaction was widely recognized as a hazard by geotechnical engineers. Most

fills were placed rapidly and in a loose condition to build military bases during World War II, port facilities, and shoreline communities like Alameda and Bay Farm Island. Probabilities of liquefaction in these areas range from 0.2 to ~0.5 for a **M**7.0 earthquake, and decrease to 0.1 to ~0.4 for a **M**6.7 earthquake. By contrast, liquefaction probabilities for both magnitudes are less than 0.05 for Holocene alluvial fan deposits, which underlie much of the remaining adjacent flat-lying urban area.

The impact of the uncertainty of the earthquake magnitude is particularly significant for areas underlain by the Holocene alluvial fan deposits. The extent of the liquefaction area decreases in the northern part of the study area and north of the fault segment boundary when the magnitude decreases from **M**7.0 to **M**6.7. Examination of the ground motions predicted in figure 6a suggests that this impact is mostly caused by a decrease in seismic demand of 16 % associated with the magnitude scaling factor. The decrease in seismic demand caused by the decrease in PGA is only 3 %.

The high probability of liquefaction adjacent to outcrops of Merritt Sand is an interesting feature of the greater Oakland area maps. These "aureoles" are created by the soil nonlinearity that was incorporated into the Boore and Atkinson (2008) ground-motion prediction equation. Inspection of figure 6b indicates that PGA decreases significantly when V_{S30} decreases from 300 m/s to 180 m/s. The Merritt Sand coincidentally has an average shear-wave velocity of 311 m/s (Holzer and others, 2005a). As one moves away from the Merritt Sand outcrop area into the fill area, the thickness of the younger bay mud and artificial fill generally increase. Both units have very low shear-wave velocities and V_{S30} in areas underlain by them approaches 180 m/s. Thus, the "aureoles" are an artifact of the combination of the systematic changes in V_{S30} and the manner in which V_{S30} is incorporated into the Boore and Atkinson (2008) ground-motion prediction equation.

IMPLICATIONS AND DISCUSSION

Liquefaction during a repeat of the 1868 Hayward Fault earthquake is predicted to be significantly more widespread in the greater Oakland area than in the northern Santa Clara Valley. The cause of the higher liquefaction hazard in the greater Oakland area is the very susceptible 57 km^2 of sandy artificial fill that were placed along the east bay shore after 1868. Recognition of the liquefaction hazard of these fills is not new. Liquefaction scenarios for a repeat of the 1906 **M**7.8 earthquake also indicated that the hazard posed by these fills is high (Holzer and others, 2006). Their high susceptibility also has been flagged by regional liquefaction susceptibility maps, most recently by Witter and others (2006)

In the greater Oakland area, probabilities of surface manifestations of liquefaction in areas underlain by sandy artificial fill (af) range from 0.2 to ~0.5 for a **M**7.0 event, and decrease to 0.1 to ~0.4 for a **M**6.7 event. Probabilities are less than 0.05 in the Holocene alluvial fan deposits for both magnitudes. Probabilities are based on a regionally conservative water-table depth of 1.5 m, although the water table in the area of sandy artificial fill is stabilized at approximately the mean water level of San Francisco Bay at an average depth of 1.6 m.

In the northern Santa Clara Valley, liquefaction probabilities are highest along the two major drainages, Coyote and Guadalupe Creeks. Probabilities are as high as 0.2 for an **M**7.0 earthquake and a shallow 1.5 m water table depth. If the Hayward Fault earthquake were to occur when the water table is below its historically shallowest level, probabilities would be lower. Probabilities for a water table depth of 5 m would remain greater than 0.1 along Coyote Creek for the **M**6.7 earthquake. Probabilities are less than 0.05 in the other Holocene alluvial fan deposits for both magnitudes.

The impact of changing the earthquake magnitude on liquefaction probabilities reflects how magnitude is used to calculate the liquefaction factor of safety, which is the basis for estimating liquefaction potential in our model. In the Seed-Idriss simplified procedure, magnitude is a surrogate for earthquake duration and is used to adjust seismic demand though the magnitude scaling factor (see *Liquefaction Prediction*). As noted before, when the earthquake magnitude increases from 6.7 to 7.0, the magnitude scaling factor increases seismic demand by 16 % while the PGA values estimated by Boore and Atkinson (2008) increase demand by only 3% (at 5 km from the fault and V_{S30} = 235 m/s site condition).

Acknowledgments: We thank James J. Lienkaemper and John C. Tinsley, III, for their reviews of this manuscript.

REFERENCES

Boore, D.M., and Atkinson, G.M., 2008, Ground-motion prediction equations for the average horizontal component of PGA, PGV, and 5 %-damped PSA at spectral periods between 0.01 s and 10.0 s: Earthquake Spectra, v. 24, no. 1, p. 99-138.

Holzer, T.L., ed., 1998, The Loma Prieta, California, earthquake of October 17, 1989 – Liquefaction: U.S. Geological Survey Professional Paper 1551-B, 314 p. http://pubs.usgs.gov/pp/pp1551/pp1551b/

Holzer, T.L., 2008, Probabilistic liquefaction hazard mapping, in Proceedings of the 4th Geotechnical Earthquake Engineering and Soil Dynamics, Sacramento, CA, American Society of Civil Engineers Geotechnical Special Publication 181, p. 1-32.

Holzer, T.L., Bennett, M.J., Noce, T.E., Padovani, A.C., and Tinsley, J.C., III, 2002, Liquefaction hazard and shaking amplification maps of Alameda, Berkeley, Emeryville, Oakland, and Piedmont: A digital database: U.S. Geological Survey Open-File Report 02-296. http://pubs.usgs.gov/of/2002/of02-296/

Holzer, T.L., Bennett, M.J., Noce, T.E., Padovani, A.C., and Tinsley, J.C., III, 2006a, Liquefaction hazard mapping with LPI in the greater Oakland, California, area: Earthquake Spectra, v. 22, no. 3, p. 693-708.

Holzer, T.L., Bennett, M.J., Noce, T.E., and Tinsley, J.C., III, 2005a, Shear-wave velocity of surficial geologic sediments in Northern California: Statistical distributions and depth dependence: Earthquake Spectra, v. 21, no. 1, p. 161-177.

Holzer, T.L., Blair, J.L., Noce, T.E., and Bennett, M.J., 2006b, Predicted liquefaction of east bay fills during a repeat of the 1906 San Francisco earthquake: Earthquake Spectra, v. 22, no. S2, p. S261-S278.

Holzer, T.L., Noce, T.E., and Bennett, M.J., 2008, Liquefaction hazard maps for three earthquake scenarios for the communities of San Jose, Campbell, Cupertino, Los Altos, Los Gatos Milpitas, Mountain View, Palo Alto, Santa Clara, Saratoga, and Sunnyvale--northern Santa Clara County, California: U.S. Geological Survey Open-File Report 2008-1270. http://pubs.usgs.gov/of/2008/1270/

Holzer, T.L., Noce, T.E., and Bennett, M.J., 2009, Scenario Liquefaction Hazard Maps of Santa Clara Valley, Northern California: Seismological Society of America Bulletin, v. 99, no. 1, p. 367-381.

Holzer, T.L., Padovani, A.C., Bennett, M.J., Noce, T.E., and Tinsley, J.C., III, 2005b, Mapping NEHRP V_{S30} site classes: Earthquake Spectra, v. 21, no. 2, p. 353-370.

Iwasaki, T., Tatsuoka, F., Tokida, K.-i., and Yasuda, S., 1978, A practical method for assessing soil liquefaction potential based on case studies at various sites in Japan, in Proceedings of the 2nd International conference on microzonation, San Francisco, p. 885-896.

Lawson, A.C., ed., 1908, The California Earthquake of April 18, 1906: Report of the State Earthquake Investigation Commission: Washington, D.C., Carnegie Institution of Washington Publication no. 87, v. 1, pt. 1, 192 p.

Lienkaemper, J.J., Williams, P.L., McFarland, F.S., and Caskey, J.S., 2009, The Hayward Fault: Its past large earthquakes and ongoing creep: This volume.

Leon, E., Gassman, S.L., and Talwani, P., 2006, Accounting for soil aging when assessing liquefaction potential: Journal of Geotechnical and Geoenvironmental Engineering, v. 132, no. 3, p. 363-377.

Obermeier, S.F., Jacobson, R., Smoot, J., Weems, R.E., Gohn, G.S., Monroe, J.E., and Powars, D.S., 1990, Earthquake-induced liquefaction features in the coastal setting of South Carolina and in the fluvial setting of the New Madrid seismic zone: U.S. Geological Survey Professional Paper 1504, 44 p.

Rix, G.J., and Romero-Hudock, S., 2007, Liquefaction potential mapping in Memphis and Shelby County, Tennessee: Unpublished Report to the U.S. Geological Survey, Denver, CO, 27 p. http://earthquake.usgs.gov/regional/ceus/products/download/Memphis_LPI.pdf

Robertson, P.K., and Wride (Fear), C.E., 1998, Evaluating cyclic liquefaction potential using the cone penetration test: Canadian Geotechnical Journal, v. 35, no. 3, p. 442-459.

Seed, H.B., Tokimatsu, K., Harder, L.F., and Chung, R.M., 1985, Influence of SPT procedures in soil liquefaction resistance evaluations: Journal of Geotechnical Engineering, v. 111, no. 12, p. 1425-1445.

Suzuki, Y., Tokimatsu, K., and Koyamada, K., 2003, Correlation between soil liquefaction during earthquakes and CPT data: Journal of Structural and Construction Engineering, v. 571, no. September, p. 95-102.

Toprak, S., and Holzer, T.L., 2003, Liquefaction potential index: Field assessment: Journal of Geotechnical and Geoenvironmental Engineering, v. 129, no. 4, p. 315-322.

Wentworth, C.M., and Tinsley, J.C., 2005, Tectonic subsidence and cyclic Quaternary deposition controlled by climate variation, Santa Clara Valley, California [abs.]: Geological Society of America, Abstracts with Programs, v. 37, no. 4, p. 59.

WGCEP, 2003, Earthquake probabilities in the San Francisco Bay region 2002-2032: U.S. Geological Survey Open-File Report 03-214.

Witter, R.C., Knudsen, K.L., Sowers, J.M., Wentworth, C.M., Koehler, R.D., and Randolph, C.E., 2006, Maps of Quaternary deposits and liquefaction susceptibility in the central San Francisco Bay region, California: U.S. Geological Survey Open-File Report 06-1037. http://pubs.usgs.gov/of/2006/1037/

Youd, T.L., and Hoose, S.N., 1978, Historic ground failures in Northern California triggered by earthquakes, U.S. Geological Survey Professional Paper 993, 177 p. http://pubs.usgs.gov/pp/1978/pp0993/

Youd, T.L., Idriss, I.M., Andrus, R.D., Arango, I., Castro, G., Christian, J.T., Dobry, R., Finn, W.D.L., Harder, L.F., Jr., Hynes, M.E., Ishihara, K., Koester, J.P., Liao, S.S.C., Marcuson, W.F., III, Martin, G.R., Mitchell, J.K., Moriwaki, Y., Power, M.S., Robertson, P.K., Seed, R.B., and Stokoe, K.H., II, 2001, Liquefaction resistance of soils: Summary report from the 1996 NCEER and 1998 NCEER/NSF workshops on evaluation of liquefaction resistance of soils: Journal of Geotechnical and Geoenvironmental Engineering, v. 127, no. 10, p. 817-833.

Yu, E., and Segall, P., 1996, Slip in the 1868 Hayward earthquake from the analysis of historical triangulation data: Journal of Geophysical Research, v. 101, no. B7, p. 16,101-16,118.